Journal of Basic and Environmental Sciences, 6 (2019) 104-111

ISSN
Online: 2356-6388
Print: 2536-9202

Research paper Open Access

Photocatalytic degradation of methylene blue dye using metal doped TiO_2 under Visible Light Irradiation

M. M. Mokhtar, W. A. A. Bayoumy, Samar M. Said, M. A. Mousa
Chemistry Department, Faculty of Science, Benha University, Benha, Egypt

Abstract

The paper details with the preparation and physicochemical characterization of nano TiO_2 doped with Fe and Cu produced by the sol-gel method using titanium tetra-isopropoxide as the precursor of titania as well as iron or cupper nitrates as dopant sources. The synthesized samples were characterized using XRD, FT-IR, surface texturing, UV-visible and SEM techniques. The photocatalytic activity of the prepared samples was studied using the photocatalytic degradation of methylene blue dye (MB). The Fe-TiO_2 showed the best result as the total removal of the dye was **91.75**% at pH 7.5 at the dye concentration of 5 ppm for 3 h.

Keywords: Titanium dioxide; Sol-gel; Fe and Cu dopant; photocatalyst; Visible light illumination.
Received; 5 Sept. 2018, Revised form; 25 Dec. 2018, Accepted; 25 Dec. 2018, Available online 1 April 2019

1. Introduction

Environmental issues increasingly attracted more attention of the public as the development of the urbanization. More and more indoor pollutants appear in indoor air owing to the poorly controlled contaminated sources [1].

In recent decades, the problem of industrial contamination of the atmosphere with organic compounds has become very important. One of the most pervasive problems affecting people throughout the world is inadequate access to clean water and sanitation. Problems with water are expected to grow worse in the coming decades, with water scarcity occurring globally, even in regions currently considered water-rich [2].

Many methods have been described for removal contamination from wastewater. These methods include adsorption [3], coagulation–flocculation [4], chemical oxidation (chlorination, ozonization, etc.) [5], electrooxidation [6] or electrocoagulation [7] and photodegradation [8]. Chemists differentiate between conventional oxidation e.g., with O_2, O_3, Cl_2, or KMnO4 and Advanced Oxidation Process's (AOPs) as; combinations of (O_3), light, and hydrogen peroxide (H_2O_2).

From all advanced oxidation and reduction processes, heterogenous photo-catalysts is common to be used as an effective process for dye destroying, and photocatalytic water splitting, which is mainly depend on semiconductor oxides (e.g., TiO_2) [9]. Heterogeneous photocatalysis has gained much attention toward the degradation of water pollution since this photocatalyst can achieve a complete mineralization in photocatalysis degradation process of organic pollutant. Heterogeneous photocatalysis is the process basically based on generation of the hydroxyl radical which is highly oxidizing agents [10]. This hydroxyl radical will oxidize the organic pollutants into harmless products. The combination between semiconductor photocatalyst and light sources is the key process of photodegradation.

Titanium dioxide (TiO_2) is one among the semiconductor materials that widely used by researchers due to the chemically stable, low cost, non-toxic, reusable and its high photocatalytic activity [11, 12]. This material consists of wide band gaps between 3.0 and 3.2 eV which require only UV light irradiation to utilize the activation. Thus, the limit of its photocatalysis process is restricted to only 4% of the UV originated from the solar spectrum reaches earth [13, 14]. Due to two important aspects TiO_2 cannot be used for practical applications. First one is the fast recombination rate of photo-generated electrons and holes causing low quantum efficiency and the second one is that TiO_2 can only be activated by UV light due to its large band gap [15]. The limitations of TiO_2 can overcome by modifying TiO_2 surface with doping of noble metals/ metal ions/ anions and synthesis of reduced form of TiO_2 photocatalyst [16] or preparation of composite materials [17], coupling TiO_2 with another semiconductor having a favorable band gap and doping TiO_2 with transition metals [18].

Transition metal ion especially Fe (III) dopant has more advantages as it fits easily into titanium dioxide lattice due to the similarity in ionic radius between titanium (IV) (0.745 Å) and that of Fe (III) (0.69Å) [19]. Besides, iron can act as both hole and electron traps and as recombination centers for the electron-hole pairs if ion concentrations are large [20]. Also, Cu and Ti ionic radii (0.72 Å for Cu and 0.69 Å for Ti) allows the interstitial incorporation of the dopant into the titania network [21].

In this work, Fe and Cu-doped titanium dioxide nanoparticles were synthesized and tested for their potential use in advanced water treatment applications under visible light. The prepared TiO_2 particles were characterized using UV-vis. absorption, XRD, FT-IR and SEM techniques. The photocatalytic activities of the

synthesized nano particles were investigated for methylene blue (MB) degradation under visible light irradiation. MB is selected as a model dyeing pollutant because it is one of the most important commercial dyes, has a very short excited-state lifetime, and is stable to visible and near UV light [22]

2. Experimental

2.1 Materials

Titanium (IV) isopropoxide (98%) was purchased from Acros organics New jersey, USA, copper (II) nitrate (Trihydrate) ($Cu(NO_3)_2.3H_2O$) 99% was purchased from S D Fine-Chem Limited India, ferric nitrate ($Fe(NO_3)_3.9H_2O$) 98% was purchased from Oxford laboratory reagent India, absolute ethyl alcohol, 99.8% and methylene blue dye ($C_{16}H_{18}ClN_3S.3H_2O$) were purchased from Aldrich.

2.2 Synthesis of the photocatalysts

2.2.1 Synthesis of pure TiO_2 photocatalyst

Pure TiO_2 was synthesized by using a sol- gel method, where 18.74 ml of titanium(IV) isopropoxide dissolved in 87.45 ml of ethanol was mixed with 14.58 ml of dist. H_2O. The solution was stirred in a flask at room temperature for four hours. The precipitated powder was then filtered and dried in an oven at 90ºC for two hours. After that, the powder was calcinated at five hundred degree for an hour. Finally, the obtained TiO_2 sample was grounded very well in a mortar.

2.2.2 Synthesis of Fe-TiO_2 and Cu-TiO_2 photocatalysts

Doped Fe-TiO_2 was synthesized by using the sol- gel method, where 10.53 ml of Titanium(IV) isopropoxide dissolved in 49.14 ml of ethanol was mixed with 8.19 ml of dis- H_2O and 0.4396 g of ferric nitrate ($Fe(NO_3)_3.9H_2O$) 98%. The solution stirred in a flask at room temperature for four hours, during this time a powder of Fe-TiO_2 was formed. The solution was filtered and the powder obtained was dried at room temperature. The powder was then calcinated at 500ºC for one hour. The obtained sample Fe-TiO_2 was grounded very well in an agate mortar.

The same synthetic process and the same conditions were used to prepare Cu-dopedTiO_2 photocatalyst.

2-3. Characterization methods

Powdered X-ray diffraction (XRD) patterns were performed at room temperature on a Philips X'Pert Pro Super diffractometer Diano (Diano Corporation, USA) using Co K_α radiation (λ = 1.79 Å), energized at 45 kV, and 10 mA and in the range from $2\theta = 5$ to 80º at a scan rate of $5°min^{-1}$.

Scanning electron microscopy (SEM), (JEOL JEM-6510 LV) was used to examine the morphology and the dimension of the investigated samples using conductive carbon paint.

The FT-IR spectra of the samples were recorded using KBr pellets in the range of 4000–400 cm^{-1} on FT-IR Thermo scientific Nicolet iS10- spectrometer.

The optical measurements were carried in the wavelength range of 200 –800 nm using diffuse reflectance ultraviolet–visible spectroscopy (UV–vis DRS) by Perkin Elmer Lamda-900 spectrophotometer using $BaSO_4$ as a reflectance standard sample.

2.4. Photocatalytic activity measurements

The photo-degradation of methylene blue dye was studied in a simple photo-reactor (which include a visible lamb of 160 watt emitting light of λ >420 nm). Aqueous suspensions of MB (100 ml) were placed in a glass beaker, into which an appropriate amount of pure or doped TiO_2 nanoparticles (the catalyst) was added. Prior to irradiation, the suspension was magnetically stirred in the dark for approximately 1 h to be sure that the suspension is in adsorption and desorption equilibrium. The photocatalyst was separated from the heterogeneous solution at different time intervals by centrifuging the solution; before any absorbance measurement, at 3000 rpm for 15 min to remove the catalyst particles completely. The decomposition of MB dye was monitored by the UV–vis spectrophotometer using a Shimadzu UV-2350 spectrophotometer.

3. Results and discussion

3.1. XRD investigation

XRD patterns of pure TiO_2 and doped TiO_2 samples are shown in Figure 1. The Cu-TiO_2 sample exhibited an anatase (tetragonal $D_{4h}I4_1/amd$) structure with peaks at 25.5°, 37.9°, 48.045° and 54.1corresponding to the crystal planes of (101), (004), (111), (200) and (105), respectively (JCPDS No. 21-1272). But, the XRD of pure and Fe-doped TiO_2 samples showed beside the anatase phase the appearance of a brookite phase at 30.7∘ corresponding to the (121) plane (JCPDS No. 76-1936). The percentage of each phase was calculated using Eq. (1) and listed in Table 1.

$$R = I_{br}(121)/[I_{br}(120) + I_{an}(101)] \quad (1)$$

Where I_{br} and I_{an} are the intensities of XRD peak planes of brookite and anatase phase, respectively.

The average crystallite size (D) of the materials investigated was calculated from the Debye-Scherrer formula [23].

$$D = 0.89\lambda / \beta \cos\theta \quad (2)$$

where D is the crystalline size, λ is the wavelength, β is the full width at half maximum intensity (FWHM-in radian), and θ is the Bragg diffraction angle (o). The values obtained are listed in Table (1) and found to be 5.9, 25.2 and 35.3 nm for undoped TiO_2, Fe-doped TiO_2 and Cu-doped TiO_2, respectively. The lattice constant values of all the studied samples were calculated by using the equation:

$$(1/d^2_{hkl}) = (h^2 + k^2 / a^2) + (l^2/c^2) \quad (3)$$

Where (hkl) are the Miller indices, (d_{hkl}) is lattice space, and (a) as well as (c) are lattice dimensions.

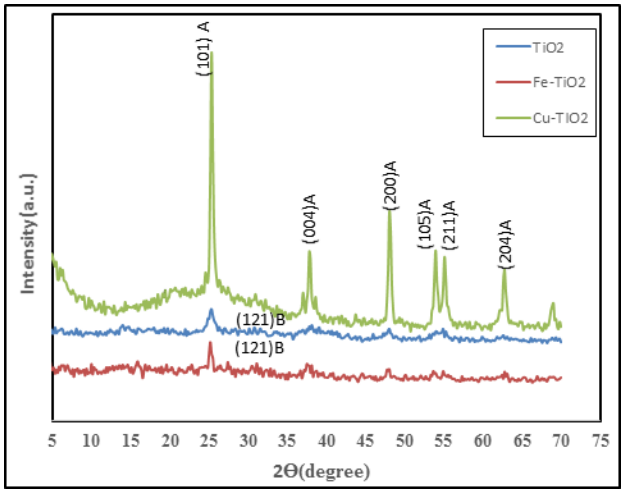

Fig (1): XRD patterns of TiO_2, Fe-TiO_2 and Cu-TiO_2 samples calcined at 500°C.

Table (1): XRD data of the investigated samples

Sample	Anatase phase percentage	Brookite phase percentage	Crystal size(nm)	Lattice parameter(Å)
TiO_2	62.4	37.6	5.9	a=3.786 c=9.458
Fe-TiO_2	61.0	39.0	25.2	a=3.783 c=9.358
Cu-TiO_2	100	------	35.3	a=3.779 c=9.490

3.2 Fourier transform infrared spectroscopy (FT-IR)

FT-IR spectra of the samples investigated are shown in Fig. 2 and the main bands are listed in Table 2. The spectra show a strong absorbance band appeared in the range of 400–600 cm^{-1}. This band is assigned to the stretching vibration of Ti- O- Ti bond referring to the creation of TiO_2. The shift observed in this band confirms the incorporation of the dopants into TiO_2 lattice. Another vibration band ranged from 1622 cm^{-1} to 1632 cm^{-1} corresponding to the O-H bending vibration for H_2O molecule was also observed. This might be attributed to the bending mode of adsorbed H_2O molecules. The vibration band observed at ~ 3400 cm^{-1} can be assigned for adsorbed H_2O molecules [24]. The shift occurred in the vibration bands of doped TiO_2 is an evidence on the success of the doping process.

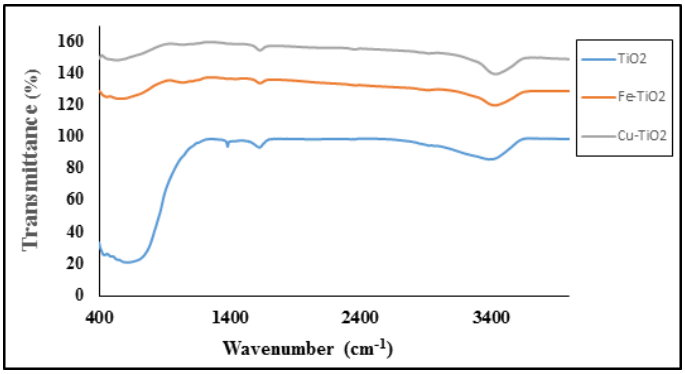

Fig (2): FT-IR spectra of TiO_2, Fe-TiO_2 and Cu-TiO_2 samples.

Table (2): Vibration modes of TiO_2, Fe-TiO_2 and Cu-TiO_2 samples

Sample	Vibration modes (Cm^{-1})	Assignments
TiO_2	646	Ti-O-Ti bending vib.
	1622	O-H bending vibration
	3383	adsorbed H_2O molecules
Fe-TiO_2	554	Ti-O-Ti bending Vib.
	1632	O-H bending vibration
	3432	adsorbed H_2O molecules
Cu-TiO_2	522	Ti-O-Ti bending vib.
	1631	O-H bending vibration
	3437	adsorbed H_2O molecules

3.2 Scanning electron microscopy (SEM)

The SEM-images of the studied samples, shown in Fig. 3, display that the shape of both undoped and doped TiO_2 samples are composed of spherical shapes of nanoparticles with different sizes. The global and uniform particles shown in Fig. 3 are coherent together.

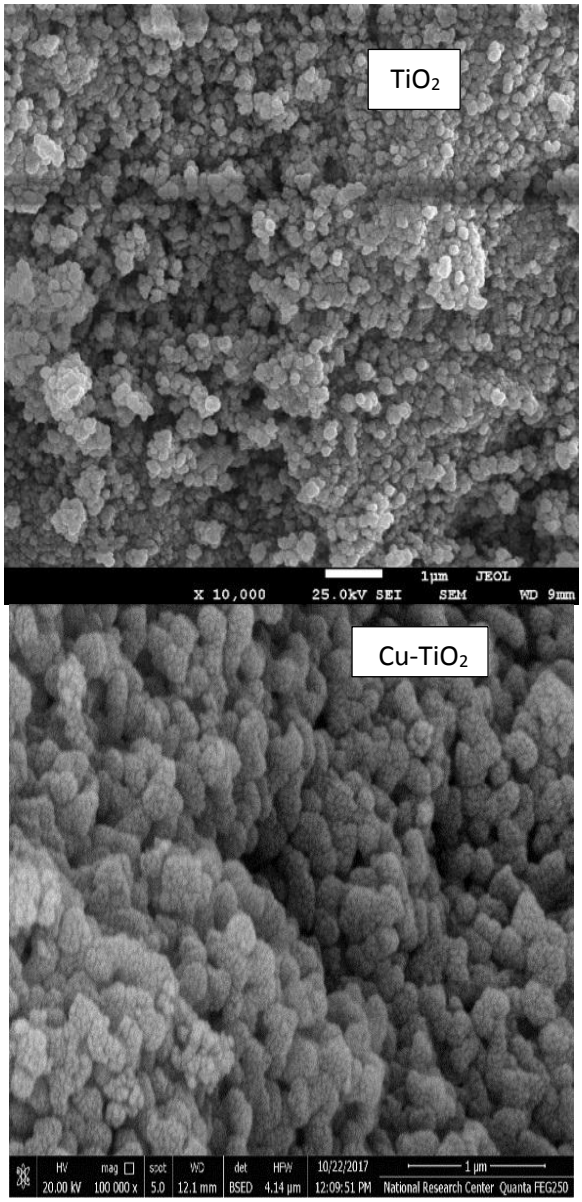

Fig. (3): SEM images of the investigated samples

3.3 Brunauer–Emmett–Teller technique (BET)

N_2 adsorption/desorption isotherms and pore size distribution (inset) of all investigated samples are shown in Fig (4). The isotherms of undoped TiO_2 and Cu-dopedTiO_2 samples show type II with H3 hysteresis loops consistent with the IUPAC classification, whereas the isotherm of Fe-dopedTiO_2 displays type IV with H1 hysteresis. The H3 hysteresis characterizes aggregates of plates-likes or slit shaped type of pores whereas H1 depicts open ended cylindrical types of pores. The surface properties of synthesized samples determined by N_2 adsorption-desorption measurements are listed in Table (3). Apparently, the Fe-TiO_2 catalyst indicates the highest S_{BET} as well as the highest pore radius (4.3-4.4 nm) and volume values than those of other catalysts. Also, the increase in pore volume and radius of Fe-TiO_2 catalyst reflects the deep deposition of Fe atoms inside the TiO_2 pores with widening the pore mouth as well as its depth. Contrarily, the Cu-TiO_2 catalyst that showed the lowest S_{BET} between the catalysts indicates the lowest pore volume (72.9 ml g^{-1}) and radius (2.9 nm) values even lower than the corresponding ones in the pristine TiO_2 catalyst (89.9 ml g^{-1} and 4.5 nm), advocating the well dispersion of Cu atoms inside the TiO_2 pores. From which it can be seen that the surface area increases in the order: Fe-TiO_2 > Cu-TiO_2 > pure TiO_2. On the other hand, the pore diameter decreases in the order: Cu-TiO_2 < Fe-TiO_2 < pure TiO_2.

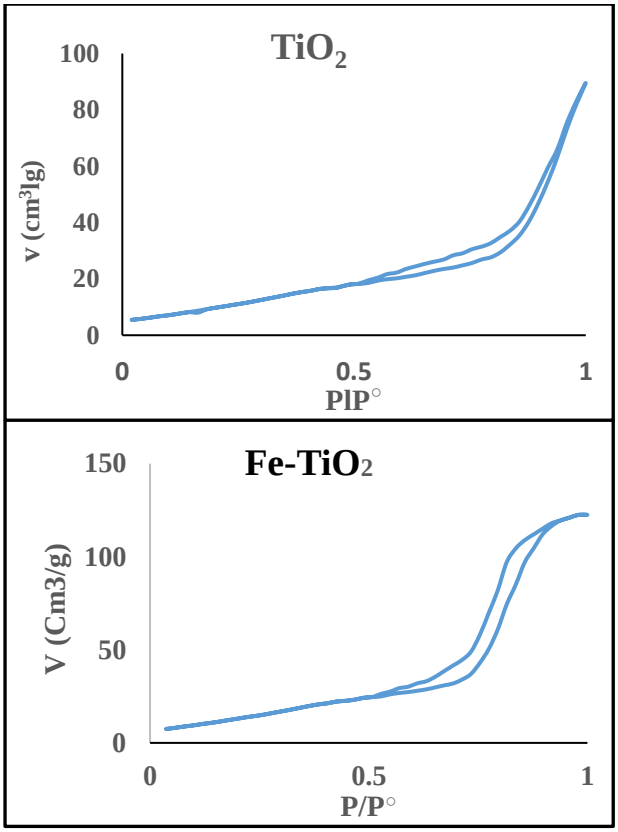

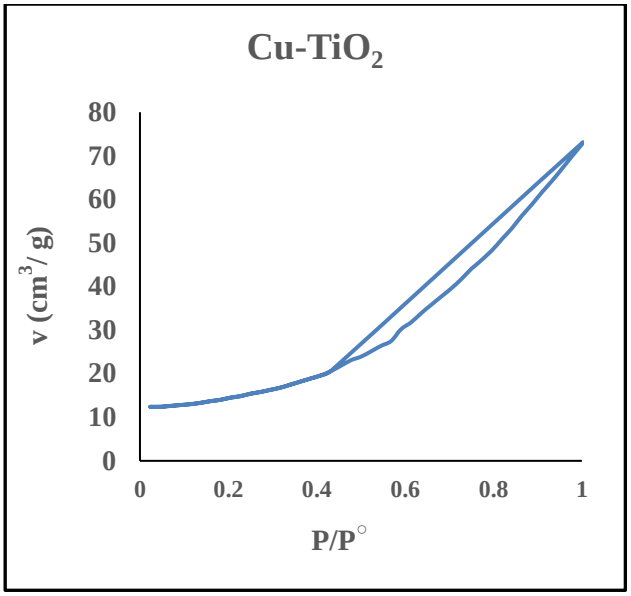

Fig (4): N_2 adsorption-desorption isotherms of the samples.

Table (3): Surface parameters of the prepared samples.

Sample	Surface area S_{BET} (m^2/g)	Total pore volume V_P (ml/g)	Average pore radius r (nm)
TiO_2	40.2	89.544	4.5
Fe-TiO_2	55.7	122.5	4.4
Cu-TiO_2	49.9	72.9	2.9

3.4 UV-Visible spectroscopy

Light absorption properties of the synthesized samples were studied by UV–vis spectroscopy. Fig. (5) represents the Kubelka–Munk function F(R), which is proportional to the absorption of radiation by the samples. For all the samples their maximum absorption is about 280–340 nm of wavelength. In comparison with that of undoped TiO_2 , the absorption edges of the Cu-doped TiO_2 and Fe-doped TiO_2 have shown a red shift. The shift means that each of Cu^{2+} and Fe^{3+} doping can enlarge the wavelength response range and could enhance visible-light photocatalytic activity of the TiO_2.

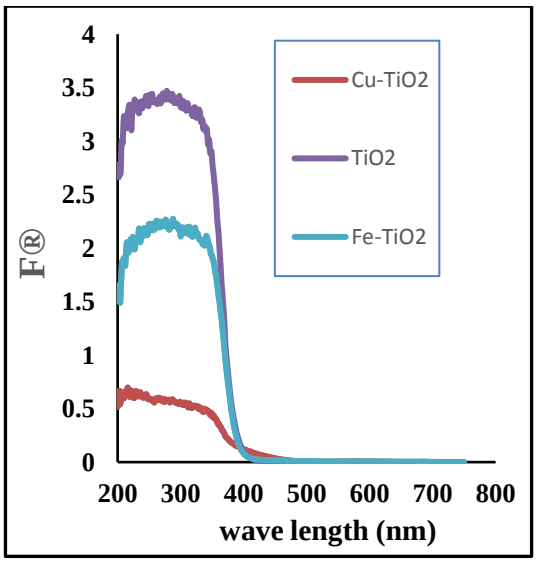

Fig (5): Optical absorption spectra of pure TiO_2, Fe-TiO_2 and Cu-TiO_2 samples.

Based on the absorption spectra, the optical band-gap was determined by using Tauc's relationship [25]

$$\alpha\eta\upsilon = B\,(\eta\upsilon - E_\gamma)^{\nu} \qquad (4)$$

Where α is the optical absorption coefficient, h is Planck, s constant, $h\upsilon$ is the photon frequency, B is a constant, E_g is the optical band gap and n is 1/2 or 2 for direct or indirect band gap semiconductor, respectively. Tauc's plot for all samples shows that band-to-band indirect transitions are more likely to occur than the direct transitions. The linear part of the plot of $(\alpha E)^2$ vs. E, Fig. 5, has been extrapolated to the α E = 0 (where E = E_g). E_g values obtained are given in Table 4. From which it can be seen that the E_g values of the doped samples are smaller than that for the pure one

Table (4): the band gab of the investigated samples

Sample	Energy gap (ev)
TiO_2	3.1
Fe-TiO_2	3.025
Cu-TiO_2	2.8

3.5 Photocatalytic results

The photo catalytic activity of the Fe-TiO_2 and Cu-TiO_2samples were examined for an aqueous solution of the MB dye with a concentration 20 ppm, pH 7.5 while using a visible lamp of 160 watt. The results obtained are illustrated in Fig. (6) showed that the total removal of the dye using Fe-doped TiO_2 is higher than that of the Cu-dopedTiO_2 sample. Therefore, we selected Fe- dopedTiO_2 sample to study the effect of different parameters (pH, catalyst dose, and dye initial concentration) upon the photocatalytic degradation of MB dye.

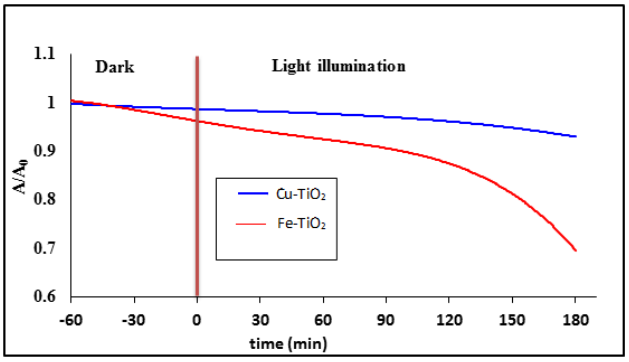

Fig (6): Photodegradation of 20 ppm MB in 1 g/L of Cu-doped TiO_2 and Fe-doped TiO_2.

3.5.1. Effect of pH

Since photocatalysis occurs at the surface, therefor the effect of pH on the degradation rate of MB using pure and doped TiO_2 samples was investigated in the pH range 2.4 to 9. The interpretation of the pH effect on the degradation process is difficult as it contains various factors such as electrostatic interactions between the catalyst surface and reaction of charged radicals such as superoxide, hydroxyl radicals, etc. molded on the catalyst surface with pollutant molecules. The results obtained are represented in Fig. 7, elaborating that highest dye removal is occurred at pH 7.5.

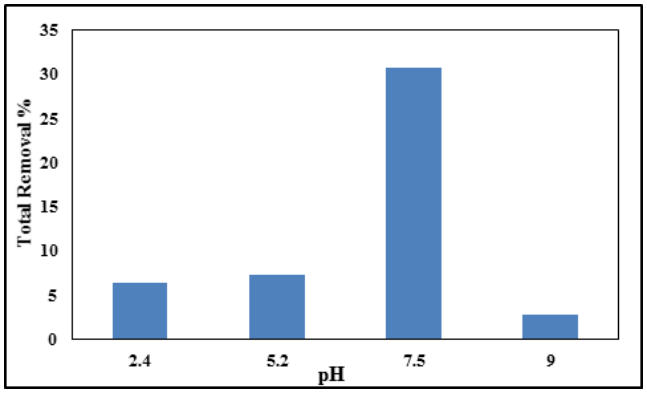

Fig. (7): pH effect on photocatalytic degradation of 20 ppm dye solution present in 1 g/L Fe-doped TiO_2 at 180 min.

3.5.2 Effect of photocatalyst load

To find the optimum amount of photocatalyst load for efficient degradation, the degradation of 20 ppm of MB dye solution was studied by varying the amount of the photocatalyst load from (0.05 to 0.20 g/50ml of dye solution) at pH 7.5 for 3 hrs. The results obtained are illustrated in Fig. 8. The optimal weight of catalyst was 0.1 g. As the weight of catalyst increased the dye degradation was not enhanced because of scavenging OH radicals via unwanted side reactions, thus a nearly complete degradation was achieved at the optimum catalyst weight (catalyst dose).

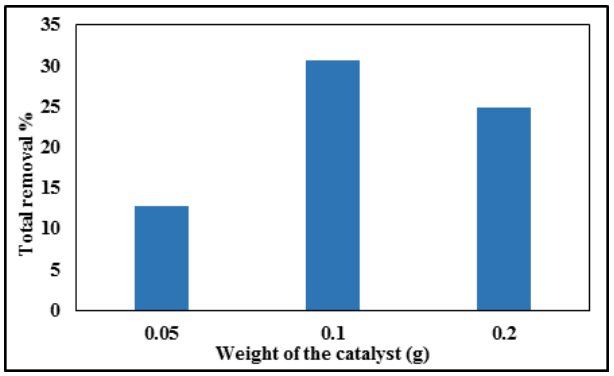

Fig. (8): Effect of Fe-doped TiO_2 photocatalyst load on the degradation of 50 ppm MB aqueous solution at pH = 7.5 for 3 h.

3.5.3. Effect of dye concentration:

The effect of dye concentrations (20, 10 and 5 ppm in 50 ml of dye solution) on the photo catalytic efficiency was studied at pH 7.5 and catalyst dose of 1 g/L. The selection of this pH is based on the optimal pH determined from the pH study and also the optimal weight determined from catalyst load study. The degradation was found to decrease with increasing the dye concentration, it was found that the increase in dye concentration had a negative effect on the photo catalytic efficiency. As at 20, 10 and 5 ppm the total removal was 30.72, 55.75 and 91.75% respectively as shown in Fig (9). This can be explained on the basis that in the high dye concentration more molecules may be adsorbed on the catalyst surface and occupying the active sites of the catalyst. And consequently, less light will be absorbed by the catalyst

causing a decrease in the concentration of $e^{/}/h^{+}$ and hence a decrease in the efficiency of the catalyst.

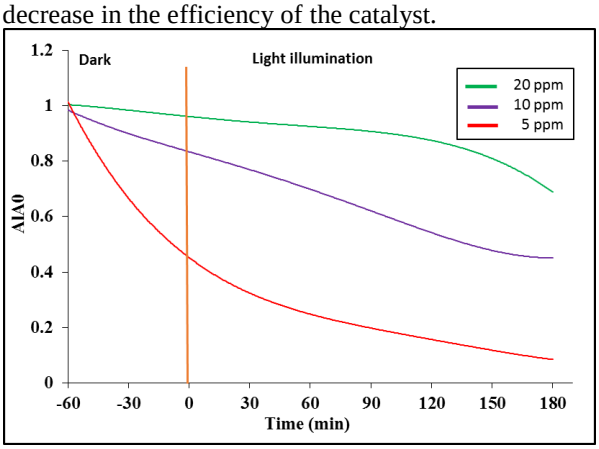

Fig (9): Effect of dye initial concentration on the degradation rate at pH=7.5 and catalyst dose of 1 g/L.

a. Effect of scavengers

As is well known, active species such as h^{+} and $^{\cdot}OH$ might play important roles in the photocatalytic oxidation process. Thus, in order to understand the photocatalytic mechanism of Fe-doped TiO_2 on MB, the active species trapping experiment were performed. Carbon tetrachloride, triethanol amine, p-benzoquinone, and isopropanol alcohol were used as the scavengers of electron (e^{-}), positive hole (h^{+}), $O_2^{\bullet}$ and $OH^{\bullet}$, respectively. The results represented in Fig. (10) show that the photocatalytic activity lowered in the presence of the scavenger according to the order: $OH^{\bullet}$> holes >electrons > $O_2^{\bullet}$. This reveals to that hydroxyl radical is the most important species in the photocatalytic process.

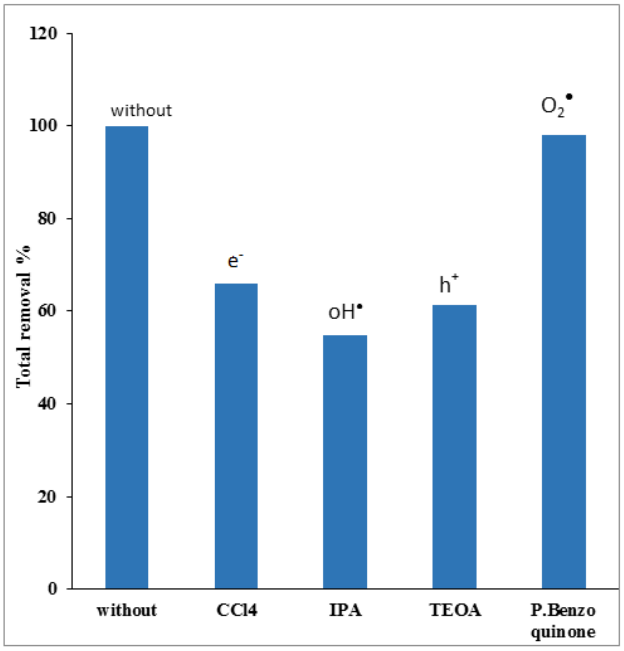

Fig (10): Effect of scavengers on the photo catalytic degradation of MB dye for Fe-TiO_2 catalyst under visible light irradiation.

4. Conclusions

In Summary, we prepared pure and metal doped TiO_2 nanoparticles using Cu^{2+} and Fe^{3+} dopant ions by sol-gel method. The samples were characterized by FT-IR, XRD, UV-Vis, BET, and SEM. The XRD patterns suggested the formation of a mixed phase (anatase and brookite) in pure TiO_2 and Fe-TiO_2 samples and only an anatase phase in Cu-TiO_2. Average crystallite size lies in the range of 5.9 – 35.3 nm and increases by introducing the dopant ions. While energy gap E_g is found to decrease from 3.19 eV for pure TiO_2 to reach 3.0, and 2.8 eV for Cu-doped TiO_2 and Fe-doped TiO_2, respectively. The surface area increases in the order Fe-TiO_2> Cu-TiO_2> TiO_2 causing an enhancement in the photocatalytic results. The photocatalytic activity improved by introducing Cu and Fe into TiO_2. The optimum conditions for the photocatalytic degradation of MB over Fe-doped TiO_2 are: pH = 7.5, catalyst dose 1 g/L and 5 ppm concentration of MB. The scavenger effect of the photocatalytic process shows a decrease in the degradation process according to the elimination of the active species in the order: $OH^{\bullet}$> holes >electrons > $O_2^{\bullet}$.

References

[1] D. Aljuboury, P. Palaniandy, H. Aziz, and F. Shaik, "Evaluating the TiO_2 as a solar photocatalyst process by response surface methodology to treat the petroleum waste water". Internat. J. Karbala Modern Sci. 1 (2015) 78-85.

[2] M. A. Shannon, Paul W. Bohn, M. Elimelech, J. G. Georgiadis, B. J. Marinas, and A. M. Mayes, "Science and technology for water purification in the coming decades". NATURE, 452 (2008) 301- 310.

[3] R. V. Kandisa, N. Saibaba, K. BeebiShaik , and R Gopinath, "Dye removal by adsorption: A review". J. Bioremediation & Biodegradation, 7 (2016) 1-4.

[4] I. A. Obiora-Okafo, and O. D. Onukwuli, "Optimization of coagulation-flocculation process for color removal from azo dye using natural polymers: response surface methodological approach". Nigerian Journal of Technology. 36 (2017) 482 – 495.

[5] E. Ebrahiem, M. N. Al-Maghrabi, and A. R. Mobarki,"Removal of organic pollutants from industrial wastewater by applying photo-Fenton oxidation Technology". Arab. J. Chem. 10 (2017) 1674–1679.

[6] A. Tiwaria, and O. Sahub,"Treatment of food-agro (sugar) industry wastewater with copper metal and salt: Chemical oxidation and electro-oxidation combined study in batch mode". Water Resources and Industry, 17 (2017) 19-25.

[7] B. K. Nandi, and S. Patel, "Effects of operational parameters on the removal of brilliant green dye from aqueous solutions by electrocoagulation", Arab. J. Chem. 10 (2017) 2961–2968.

[8] A. Pandey, P. Singh, and L. Ivengar, " Bacterial decolorization and degradation of azo dyes".Int. Biodeterior. Biodegrad. 59 (2007) 73–84.

[9] Y. Wang, L. Li, X. H. Li, and G. Li, "New insights into fluorinated TiO_2 (brookite, anatase and rutile) nanoparticles as efficient photo catalytic redox catalysts ". RSC Adv.5 (2015) 34302–34313.

[10] U.I. Gaya and A.H. Abdullah, "Heterogeneous photocatalytic degradation of organic contaminants over titanium dioxide: A review of fundamentals, progress, and problems", *J. Photochem. Photobiolo. C: Photochem. Rev.* 9 (2008) 1-12.

[11] M.A. Nawi, and S.S. Sheilatina, "Photocatalytic decolourisation of reactive red 4 dyes by an immobilised TiO_2/chitosan layer by layer system", J. Colloid Interface Sci. 372 (2012) 80-87

[12] T.K. Tseng, Y.S. Lin, Y.J.Chen, and H. Chu, "A review of photocatalysts prepared by sol-gel method for VOCs removal". International Journal of Molecular Sciences. 11(2010) 2336-2361.

[13] J.H. Castillo-Ledezma, and J. L. S. Salas, "Effect of pH, solar irradiation, and semiconductor concentration on the photocatalytic disinfection of Escherichia coli in water using nitrogen-doped TiO_2". European Food Research and Technology. 233 (2011) 825-834.

[14] Y. Cong, J. Zhang, F. Chen and M. Anpo."Synthesis and characterization of nitrogen-doped TiO_2 nano photocatalyst with high visible light activity". J. Phys. Chem, 111 (2007) 6976-6982.

[15] MI. Litter, "Heterogeneous photocatalysis: transition metal ions in photocatalytic systems". Appl Catal B: Environ 23(1999) 89-114.

[16] W. Choi, A. Termin and MR. Hoffmann, "The role of metal ion dopants in quantum-sized TiO_2: correlation between photoreactivity and charge-carrier recombination dynamics". J Phys Chem; 98(1994) 13669-13679.

[17] F. Maraschi, M. Sturini , A. Speltini , L. Pretali , A. Profumo, A. Pastorello , V. Kumar, M. Ferretti, and V. Caratto, "TiO_2-modified zeolites for fluoroquinolones removal from waste waters and reuse after solar light regeneration", J. Environ. Chem. Eng. 2 (2014) 2170–2176.

[18] C. Wang, C. Bottcher, D. Bahnemann and J. Dohmann, "A comparative study of nanometer sized Fe (III)-doped TiO_2 photocatalysts: Synthesis, characterization and activity". J. Mat. Chem. 13 (2003) 2322-2329.

[19] X. Zhang, M. Zhou, and L. Lei, "Co-deposition of photocatalytic
Fe-doped TiO_2 coatings by MOCVD". Catal Commun. 7 (2006):427-31.

[20] J. Zhu, W. Zheng, B. He, J. Zhang and M. Anpo, "Characterization of Fe-TiO_2 photocatalysts synthesized by hydrothermal method and their photocatalytic reactivity for photodegradation of XRG dye detected in water". J Mol Catal A: Chem. 216 (2004) 35-43.

[21] W. Yang, D. Wubiao, L. Bo, C. Xidong, Y. Feihua, and G. Jianping, "The effects of doping copper and mesoporous structure on photocatalytic properties of TiO2" Journal of Nanomaterials, 1 (2014) 1- 7.

[22] H.G. Yu, J.G. Yu, S.W. Liu, and S. Mann," Template-free hydrothermal synthesis of CuO/Cu_2O composite hollow microspheres", Chem. Mater. 19 (2007)4327–4334.

[23] W. Yao, W. Zhuang and X. Ji Wang, "Solid state synthesis of $Li_4Ti_5O_{12}$ whiskers from TiO_2-B". Mat. Res. Bull. 75 (2016) 204-210.

[24] P. A. Gerakines, W. A. Schutte, J. M. Greenberg, and E. F. van Dishoeck, "The infrared band strengths of H_2O, CO and CO_2 in laboratory simulations of astrophysical ice mixtures" Astro-ph. 1 (1995) 1-16.

[25] H. K. Jeong, Y. P. Lee, R. J. Lahaye, M. H. Park, K. H. An, I. J. Kim, C. W. Yang, C. Y. Park, R. S. Ruoff, and Y. H. Lee, "Evidence of graphitic AB stacking order of graphite oxides". J. Am. Chem. Soc., 3 (2008) 1362-1366.